Neutron Off-Plane Scattering of Aligned Membranes. I. Method of Measurement

Lin Yang, Thad A. Harroun, William T. Heller, Thomas M. Weiss, and Huey W. Huang
Physics Department, Rice University, Houston, Texas 77251-1892 USA

ABSTRACT We describe a method of measuring neutron scattering of aligned membranes with the momentum transfer oriented parallel or partly perpendicular to the plane of the membranes. The method obtains the complete information for the structures within fluid membranes obtainable by scattering. Data from alamethicin- and magainin-induced pores are presented. Although the in-plane scattering curves of these two peptides are similar to each other, their off-plane scattering patterns are strikingly distinct. Magainin pores exhibit intermembrane correlations.

INTRODUCTION

X-ray and neutron scattering techniques are the only methods that can probe the structures in fluid membranes directly. In the last few years we have used the techniques of in-plane scattering to detect and analyze the peptide-induced pores in membranes (He et al., 1995, 1996; Ludtke et al., 1996). In these experiments, membranes are prepared in the form of oriented lamellae in which parallel membranes are separated by water layers. The momentum transfer of scattering was oriented parallel to the plane of the membranes. This is a convenient way of detecting pores in membranes. With water replaced by D_2O, neutron scattering easily detects the water channel of the pore, because D_2O provides a strong neutron scattering contrast against peptide and lipid. However, a complete structural analysis requires a scattering pattern with the momentum transfer oriented off-plane as well as in-plane. In this and a following paper, we will show the technique of measuring off-plane scattering patterns and the theory for data analysis.

We will use the alamethicin- and magainin-induced pores to demonstrate this technique. These pores were previously detected by in-plane scattering (He et al., 1995, 1996; Ludtke et al., 1996). We will show that although the in-plane scattering curves of these two pores are somewhat similar, their off-plane scattering patterns are strikingly distinct. Furthermore, in the case of the charged peptide magainin, there are correlations between pores residing in neighboring membranes. In such cases, in-plane scattering provides only approximate information for the in-plane structures. This paper describes a method of measurement with a small-angle neutron-scattering instrument.

Received for publication 8 March 1998 and in final form 1 May 1998.

Address reprint requests to Dr. Huey W. Huang, Physics Department, Rice University, Houston, TX 77251. Tel: 713-527-4899; Fax: 713-527-9033; E-mail: huang@ion.rice.edu.

0006-3495/98/08/641/05 $2.00

SAMPLES

Sample preparation for oriented membranes has been described in detail by He at al. (1996) and Ludtke et al. (1996). Briefly, 1,2-dilauroyl-sn-glycero-3-phosphatidylcholine (DLPC), 1,2-dimyristoyl-sn-glycero-3-phosphatidylcholine (DMPC), and 1,2-dimyristoyl-sn-glycero-3-phosphatidylglycerol (DMPG) were purchased from Avanti (Alabaster, AL). Alamethicin was from Sigma (St. Louis, MO). Magainin 2 amide was a gift from Drs. M. Zasloff and W. Maloy of Magainin Pharmaceuticals (Plymouth Meeting, PA). The lipids and peptides were used as delivered. Peptide and lipid at the desired peptide-to-lipid molar ratio, P/L, were dissolved in chloroform/methanol (alamethicin) or trifluoroethanol (magainin). The solvent was removed by nitrogen purge followed by drying under vacuum. D_2O was added to the peptide-lipid film. The mixture was homogenized with a sonicator and then lyophilized. The lyophilized powder was hydrated with D_2O vapor. Six thin layers of D_2O-hydrated sample were held between seven parallel quartz plates. Hydrated peptide/lipid mixtures self-assembled into parallel bilayers separated by water (D_2O) layers. The degree of lamellar alignment was manipulated by mechanical compression and thermal annealing (Huang and Olah, 1987). The peptide orientation was monitored by oriented circular dichroism (Wu et al., 1990). The total thickness of the membranes in each sample was ~0.25 mm. The sample cross sections were ~2.6 cm in diameter.

OFF-PLANE SCATTERING GEOMETRY

In the following we will describe the scattering geometry, using a generic small-angle neutron-scattering instrument that consists of a highly collimated neutron beam and an area detector oriented perpendicular to the beam. Neutron scattering measures the Fourier transform of the scattering length density of the sample in the direction of the momentum transfer $\boldsymbol{q}$. The magnitude of $\boldsymbol{q}$ is decided by the scattering angle 2θ: $q = (4\pi/\lambda)\sin\theta$. In the detector coordinates (X, Y, Z), the components of $\boldsymbol{q}$ for a scattered beam striking the detector cell (X_c, Y_c) are $q_X = q \cos\theta \cos\phi$,

$q_Y = q \cos\theta \sin\phi$, $q_Z = -q \sin\theta$, where

$$2\theta = \tan^{-1}\frac{\sqrt{X_c^2 + Y_c^2}}{R}, \quad \phi = \tan^{-1}\frac{Y_c}{X_c}$$

as defined in Fig. 1 *A*, and R is the sample-to-detector distance.

We need to express **q** in the sample coordinates (*x, y, z*). In an in-plane scattering experiment, the plane of the membranes is oriented perpendicular to the incident beam (Fig. 1 *A*). In this case, the sample coordinate axes are the same as the detector coordinate axes, i.e., $q_x = q_X$, $q_y = q_Y$, $q_z = q_Z$. For small-angle scattering, **q** is practically parallel to the sample plane ($q_z \approx 0$; Fig. 2 *A*). Thus in-plane scattering only gives lateral structural information. In general, lipid lamellar samples are disordered within the plane of membranes. Therefore, the scattering signal is cylindrically symmetrical with respect to the q_z axis. In general, in-plane scattering patterns on the detector are concentric rings. The scattering intensity is essentially a function of $q_r = \sqrt{q_x^2 + q_y^2}$. The q_z dependence is not measured.

The purpose of off-plane scattering is to project **q** with a component perpendicular to the plane of the membranes. This is achieved by rotating the sample about the *y* axis, such that the plane of the membranes is oriented at an angle

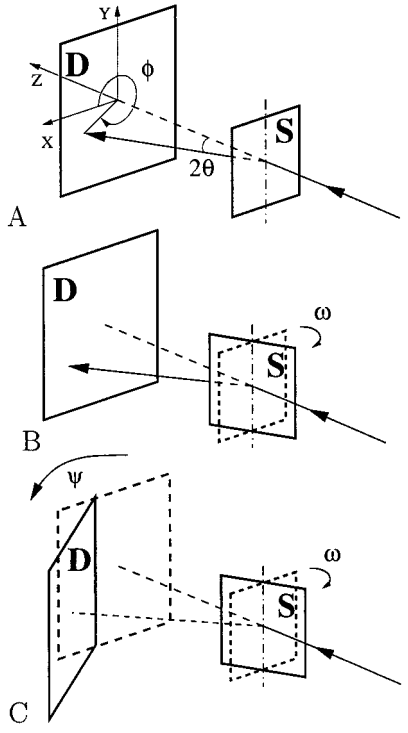

FIGURE 1 (*A*) The geometry of in-plan scattering. *S* represents the plane of multilamellar membranes and *D* the area detector, both oriented perpendicular to the incident neutron beam. The right-handed *X*, *Y*, *Z* coordinates on the detector and the corresponding sample coordinates *x*, *y*, *z* are defined facing the incident beam. (*B*) The geometry of off-plane scattering. The sample is rotated around the *y* axis by an angle ω. (*C*) The detector may be rotated to vary the coverage on the sample *q* space.

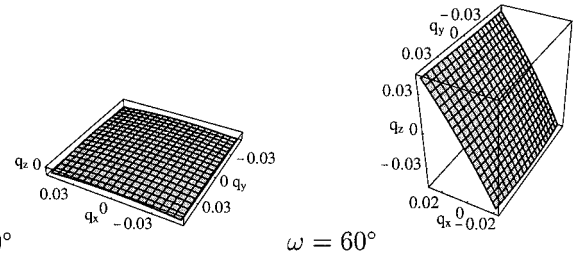

FIGURE 2 Illustrations of the sample *q* space in an in-plane scattering ($\omega = 0°$) and in an off-plane scattering ($\omega = 60°$). For the purpose of illustration, we use a detector of 20 × 20 cells. We also use a hypothetical length unit, so that the sample-to-detector distance $R = 100$ and the detector cell size is 1 × 1. The unit of *q* is 0.25 nm^{-1} for $\lambda = 0.5$ nm. (The NG-3 detector at NIST has 64 × 64 cells. The cell size is 1 cm × 1 cm. The sample-to-detector distance is 1.3–13 m, and $\lambda = 0.5$–2.0 nm.)

ω with respect to the detector (Fig. 1 *B*). The projections of **q** on the sample axes are now given by

$$q_x = \cos\omega q_X - \sin\omega q_Z = q(\cos\theta\cos\phi\cos\omega + \sin\theta\sin\omega) \tag{1.1}$$

$$q_y = q_Y = q\cos\theta\sin\phi \tag{1.2}$$

$$q_z = \sin\omega q_X + \cos\omega q_Z = q(\cos\theta\cos\phi\sin\omega - \sin\theta\cos\omega) \tag{1.3}$$

An example of $\omega = 60°$ is shown in Fig. 2 *B*. However, the structural information of fluid membranes is most clearly presented in the q_r-q_z plane. This can be achieved by converting the data directly to q_r and q_z:

$$q_r = \sqrt{q_x^2 + q_y^2} = q\sqrt{(\cos\theta\cos\phi\cos\omega + \sin\theta\sin\omega)^2 + (\cos\theta\sin\phi)^2} \tag{2.1}$$

$$q_z = q(\cos\theta\cos\phi\sin\omega - \sin\theta\cos\omega) \tag{2.2}$$

The projection of the detector space on the q_r-q_z plane is shown in Fig. 3, *A–C*, for three different values of ω. Different samples may require different coverages in the *q*-space, which can be achieved by adjusting ω.

A variation of this geometry is achieved by changing the position of the detector, for instance, by swinging the detector by an angle ψ around the vertical axis at the sample (Fig. 1 *C*). This will change the sample *q* space in another way. Fig. 3, *E* and *F*, shows two examples of different values of ψ.

DATA PROCESSING FOR OFF-PLANE SCATTERING

Besides the routine data corrections for small-angle scattering (Chen and Lin, 1987), it is necessary to correct the off-plane scattering data for sample volume and absorption. The amount of sample through which the neutron beam

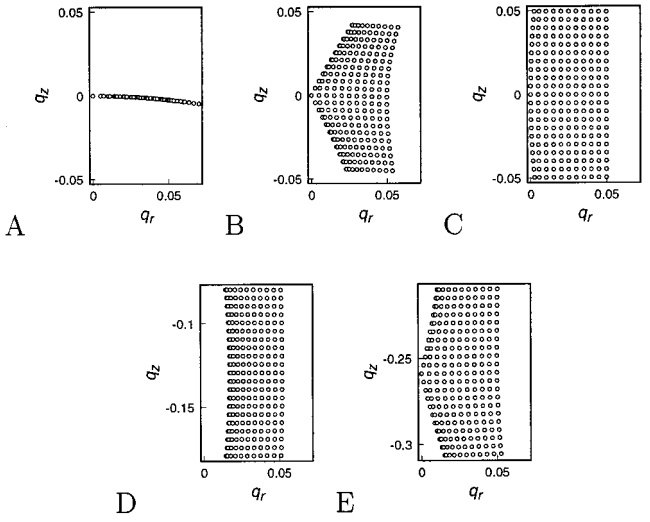

FIGURE 3 Illustrations of the sample q space in an off-plane scattering experiment using the geometry specified in Fig. 2. The three-dimensional q space is projected onto the two-dimensional q_r-q_z plane, because of the cylindrical symmetry of the scattering signal. Different coverages on the q_r-q_z plane can be achieved by varying ψ and ω (defined in Fig. 1): (*A*) ψ = 0°, ω = 0°; (*B*) ψ = 0°, ω = 60°; (*C*) ψ = 0, ω = 90°; (*D*) ψ = 15°, ω = 75°; (*E*) ψ = 30°, ω = 75°.

passes is proportional to 1/cos ω. As shown in Fig. 4 *A*, the path length of neutron through the sample depends on the angles θ and ϕ as well as ω. Let the sample's linear absorption coefficient be μ and the sample thickness be a. (The value for μa can be measured directly by a transmission measurement.) Then the total scattering intensity at (θ, ϕ), $I(\theta, \phi)$, is proportional to a correction factor given by

$$I(\theta,\phi)\propto\int_0^a \exp\left[-\frac{\mu(a-z)}{\cos\omega}\right]\cdot\exp\left(-\frac{\mu z}{\cos\alpha}\right)\frac{dx}{\cos\omega}\propto\frac{1-\exp\left[-\mu a\left(\frac{1}{\cos\alpha}-\frac{1}{\cos\omega}\right)\right]}{\mu a\left(\frac{1}{\cos\alpha}-\frac{1}{\cos\omega}\right)\cos\omega} \quad (3)$$

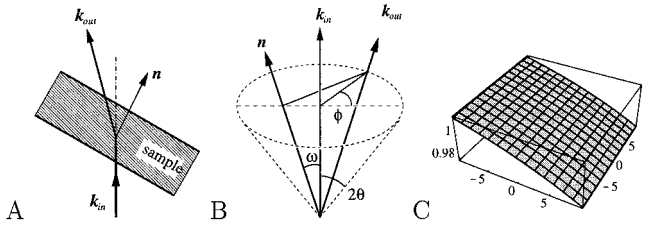

FIGURE 4 (*A*) The schematic of neutron path. In general, the scattered wave vector k_{out} is not in the plane defined by the sample normal n and the incident wave vector k_{in}. (*B*) The geometry of k_{in}, k_{out}, and n. The angle between k_{out} and n is α. The path length of neutron depends on the angle α and the depth z of the scattering point. (*C*) (cos ω) × (the correction factor) (see Eq. 3 on the detector) at ω = 60°and μa = 0.1, using the geometry specified in Fig. 2. $\mu a \approx 0.1$ is typical for our samples.

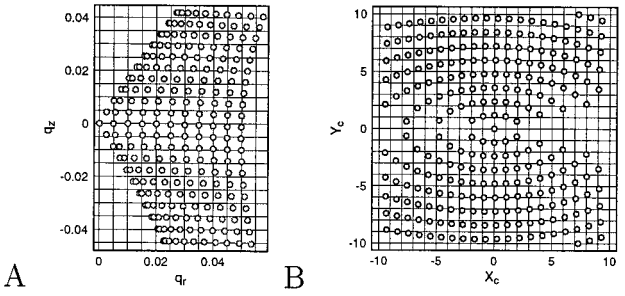

FIGURE 5 (*A*) Data taken from a regular grid on the detector are irregular on the q_r-q_z plane. (*B*) A regular grid on the q_r-q_z plane projected back onto the detector.

where α is the angle between the direction of the scattered beam, k_{out}, and the normal to the sample plane, n (Fig. 4 *B*), $\cos\alpha = \cos\omega\cos 2\theta - \sin\omega\sin 2\theta\cos\phi$. The correction factor for our samples oriented at ω = 60° is shown in Fig. 4 *C*.

Although the data points on the detector are on a regular grid, the transformed data in the sample coordinates are not (Fig. 5 *A*). For the convenience of data analysis, it is

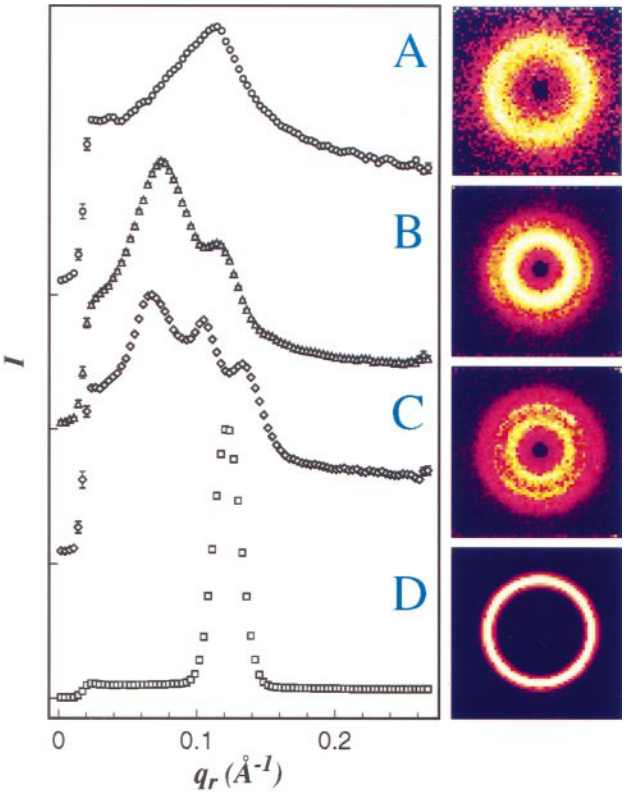

FIGURE 6 Neutron in-plane scattering of (*A*) alamethicin in DLPC bilayers at P/L = 1/20; (*B*) magainin in DMPC/DMPG (3:1) bilayers at P/L = 1/20, measured at 35°C; (*C*) sample B at 20°C; (*D*) pure DLPC sample. Samples A and D did not show temperature dependence. The right panel shows the scattering patterns on the 2D detector. The left panel shows the circularly averaged intensity I in arbitrary units versus in-plane momentum transfer q_r. The data were taken at NIST with R = 2 m and λ = 0.5 nm. The measurement time was ~10 min each.

desirable to have the data on a regular grid in the sample coordinates. This can be achieved in two ways. The obvious way is to intrapolate the irregular (q_r, q_z) data grid into a regular grid. However, a more efficient way is to start with a regular (q_r, q_z) grid and find the corresponding position (X_c, Y_c) on the detector:

$$X_c = R \tan 2\theta \cos \phi \tag{4.1}$$

$$Y_c = R \tan 2\theta \sin \phi \tag{4.2}$$

where

$$\theta = \arcsin \frac{\lambda q}{4\pi} \tag{4.3}$$

$$\phi = \arccos \frac{q_z/q + \sin \theta \cos \omega}{\sin \omega \cos \theta} \tag{4.4}$$

These coordinates in general fall between detected data points (Fig. 5 *B*). However, it is much more convenient to intrapolate from a regular coordinate to an irregular coordinate than the other way around.

In this off-plane scattering geometry, the data on the detector are symmetrical up-and-down, that is, points (X, Y) and $(X, -Y)$ correspond to the same point in the q space. On the other hand, left and right are slightly asymmetrical on the detector. The transformed data on the (q_r, q_z) plane are symmetrical with respect to the sign of q_z, $I(q_z) = I(-q_z)$, because the membranes are centrosymmetrical. The data are averaged across the symmetrical axes to improve the statistics.

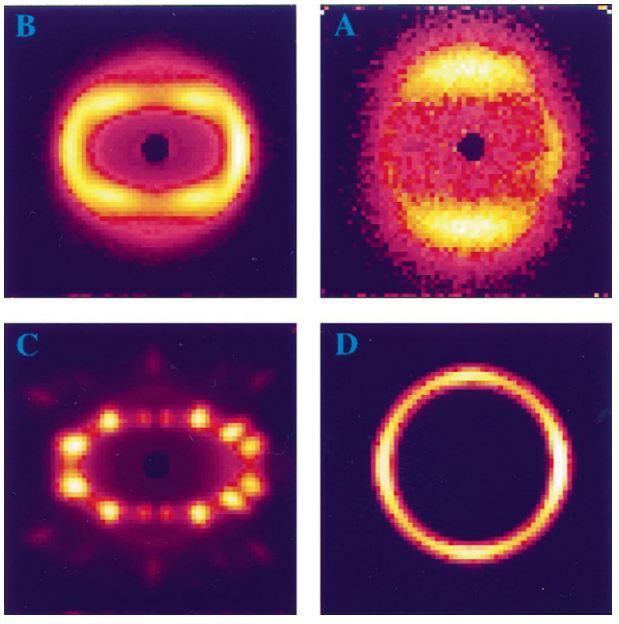

FIGURE 7 Off-plane scattering patterns on the 2D detector when the samples of Fig. 6 were rotated at $\omega = 60°$. The measurement time was 1 h each. *A* and *B* are the signature patterns of the alamethicin and magainin pores. All alamethicin and magainin samples reproduced these patterns. (*C*) The magainin sample was in a crystallline phase at 20°C. (*D*) The oily streak defects produce a circular pattern (with modulated intensities) on the detector.

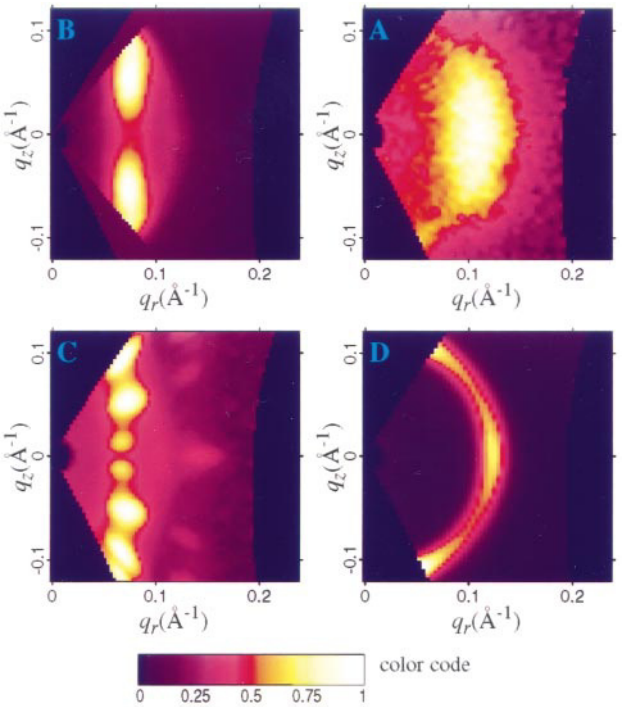

FIGURE 8 Data of Fig. 7 transformed to the q_r-q_z plane. (*A*) The q_z dependence is consistent with the form factor of an alamethicin channel (He et al., 1996). There are no intermembrane correlations. (*B*) The defect peaks are suppressed (see *D* for comparison) to show the scattering pattern of magainin. There are peaks at $q_z \approx \pm\pi/d$, where $d = 6.0$ nm is the lamellar repeat spacing. The peaks are indicative of intermembrane correlations between pores. (*C*) The diffraction pattern of a crystalline phase of the magainin-lipid mixture. The scale of this figure is the logarithm of intensity. (*D*) This diffraction pattern provides new information for the oily streak defects (Schneider and Webb, 1984). Readers may obtain the complete data from http:\\ion.rice.edu\~huang\neutron data.

DATA

We now compare the data from three different samples: alamethicin in DLPC at P/L = 1/20, magainin in a 3:1 mixture of DMPC and DMPG at P/L = 1/20, and pure DLPC. The experiments were performed at the Cold Neutron Research Facility, National Institute of Standards and Technology (NIST), using the NG-3 beamline. Selected results were reproduced at the Intense Pulsed Neutron Source (IPNS), Argonne National Laboratory, using the SAND beamline.

Fig. 6 shows in-plane scattering patterns of these three samples at 20°C and the magainin sample at 35°C. The two DLPC samples (with and without alamethicin) did not show observable temperature dependence from 20°C to 40°C. The peak of the pure lipid sample (Fig. 6 *D*) is due to oily streak defects in the lamellar phase (for a detailed discussion of the defect signals, see He et al., 1996). Because this is the result of diffraction by the defect structures, its intensity can be very strong compared to the scattering signals. Therefore, it is necessary to take the precaution of limiting the amount of defects in the sample (He et al., 1996). The defect peak also appears in the magainin sample

(Fig. 6 *B*) at a slightly smaller q, because of the differences in lipid chain length and possibly in the water (D_2O) content as well. The alamethicin and magainin peaks (Fig. 6, *A* and *B*) have been discussed previously (He et al., 1996; Ludtke et al., 1996). However, the origins of in-plane peaks are not always clear. An example is given in Fig. 6 *C*, where an interpretation based on the in-plane scattering alone would be very difficult.

This problem is now solved by off-plane scattering. Fig. 7 shows the off-plane scattering patterns on the detector produced by the previous four samples when ω was set at 60°. We see that each structure produces a unique pattern, clearly different from the others. The pattern of oily streak defects is circular. The magainin sample at 20°C is clearly crystalline. Most amazing of all, the patterns of alamethicin pores and magainin pores have distinctively different features. We have measured several alamethicin and magainin samples. All of them reproduced these unique patterns.

The scattering patterns on the q_r-q_z plane are shown in Fig. 8. These are in the form most convenient for theoretical analysis. We note that the magainin sample at 35°C shows a maximum at $q_z > 0$. This is an indication of intermembrane correlations. The data analysis will be discussed in a later paper.

CONCLUSION

Off-plane scattering provides information in addition to that of in-plane scattering. In fact, it provides the complete structural information on fluid membranes obtainable by scattering. We have shown a simple method of measuring off-plane scattering patterns using existing small-angle scattering facilities.

We thank Michael Zasloff and Lee Maloy for their generous gift of magainins, B. Hammouda and S. Krueger for assistance at the NIST, and P. Thiyagarajan at the IPNS.

This work was supported by National Institutes of Health Grant GM55203 and Training Grant GM08280, and by the Robert A. Welch Foundation. We acknowledge the support of the NIST, U.S. Department of Commerce, in providing the neutron research facilities used in this work, which was also supported by the National Science Foundation under agreement no. DMR-942310, and of the IPNS, funded by the U.S. Department of Energy, BES-Materials Science, under contract W-31-109-Eng-38.

REFERENCES

Chen, S. H., and T. L. Lin. 1987. Colloidal Solutions. *In* Method of Experimental Physics, Part B, Vol. 23, Neutron Scattering. D. Price and K. Skold, editors. Academic Press, New York. 489–543.

He, K., S. J. Ludtke, D. L. Worcester, and H. W. Huang. 1995. Antimicrobial peptide pores in membranes detected by neutron in-plane scattering. *Biochemistry.* 34:16764–16769.

He, K., S. J. Ludtke, D. L. Worcester, and H. W. Huang. 1996. Neutron scattering in the plane of membranes: structure of alamethicin pores. *Biophys. J.* 70:2659–2666.

Huang, H. W., and G. A. Olah. 1987. Uniformly oriented gramicidin channels embedded in thick monodomain lecithin multilayers. *Biophys. J.* 51:989–992.

Ludtke, S. J., W. T. Heller, T. A. Harroun, L. Yang, and H. W. Huang. 1996. Membrane pores induced by magainin. *Biochemistry.* 35: 13723–13728.

Schneider, M. B., and W. W. Webb. 1984. Undulating paired disclinations (oily streaks) in lyotropic liquid crystals. *J. Phys. France.* 45:273–281.

Wu, Y., H. W. Huang, and G. A. Olah. 1990. Method of oriented circular dichroism. *Biophys. J.* 57:797–806.